Optics Letters

# Experimental demonstration of phase-sensitive regeneration of a binary phase-shift keying channel without a phase-locked loop using Brillouin amplification

AHMED ALMAIMAN,[1,*] YINWEN CAO,[1] MORTEZA ZIYADI,[1] AMIRHOSSEIN MOHAJERIN-ARIAEI,[1] PEICHENG LIAO,[1] CHANGJING BAO,[1] FATEMEH ALISHAHI,[1] AHMAD FALLAHPOUR,[1] BISHARA SHAMEE,[1] NISAR AHMED,[1] ASHER J. WILLNER,[1] YOUICHI AKASAKA,[2] TADASHI IKEUCHI,[2] SHIGEHIRO TAKASAKA,[3] RYUICHI SUGIZAKI,[3] STEVEN WILKINSON,[4] JOSEPH D. TOUCH,[1,5] MOSHE TUR,[6] AND ALAN E. WILLNER[1]

[1]Department of Electrical Engineering, University of Southern California, Los Angeles, California 90089, USA
[2]Fujitsu Laboratories of America, 2801 Telecom Parkway, Richardson, Texas 75082, USA
[3]Fitel Photonics Laboratories, Furukawa Electric Co., 6 Yawata Kaigan-dori, Ichihara, Chiba 290-8555, Japan
[4]Raytheon Company, El Segundo, California 90245, USA
[5]Information Sciences Institute, University of Southern California, Marina del Rey, California 90292, USA
[6]School of Electrical Engineering, Tel Aviv University, Ramat Aviv 69978, Israel
*Corresponding author: Almaiman@usc.edu

Received 14 September 2016; revised 21 October 2016; accepted 23 October 2016; posted 25 October 2016 (Doc. ID 275937); published 16 November 2016

**All-optical phase regeneration of a binary phase-shift keying signal is demonstrated at 10–30 Gb/s without a phase-locked loop in a phase-sensitive amplification-based system using Brillouin amplification of the idler. The system achieves phase noise reduction of up to 56% and up to 11 dB OSNR gain at $10^{-5}$ bit error rate for the 10 Gb/s signal. The system's sensitivity to different parameters and stability is also evaluated.** 

***OCIS codes:*** (060.2360) Fiber optics links and subsystems; (070.4340) Nonlinear optical signal processing.

http://dx.doi.org/10.1364/OL.41.005434

All-optical regeneration of phase-shift-keyed (PSK) data channels is of high interest since the reduction of phase noise can significantly increase the communication system performance [1]. One promising regeneration technique is the use of phase-sensitive amplification (PSA), where the phase noise is attenuated (i.e., squeezed) during the PSA process [2].

PSA-based regeneration for phase-encoded data occurs using nonlinear wave mixing. For example, in a highly nonlinear fiber (HNLF), two pumps and a binary phase-shift keying (BPSK) data channel can mix with each to reduce the signal's phase noise, but this mixing is efficient only when the data channel is placed in the middle between the two pump lines, and the data channels as well as pumps are coherent with each other. This will result in the signal getting added with its conjugate. Therefore, the part of the signal that has a different phase from the pumps will be "squeezed," which reduces the phase noise for the BPSK channel [2–4].

A key requirement of this approach is that the pumps and the data channel must be phase-locked and coherent with each other. Various methods for meeting this requirement include: (i) using a phase-locked loop (PLL) to adjust the relative phase alignment [2–13]; (ii) using multiplication between the data channel and its delayed conjugate, which alters the data coding format [14]; and (iii) using a comb of three mutually coherent frequency lines as well as cross-phase modulation between the middle line and the data channel [15].

In this Letter, we demonstrate a phase-sensitive regeneration of a BPSK channel up to 30 Gb/s without the need for a PLL using a Brillouin amplifier (BA). A data pattern-free idler is generated in a HNLF, similar to [2–10], and the narrow bandwidth (BW) nature of the Brillouin amplifier (~25 MHz 3 dB bandwidth) [16–20] is used to amplify the idler "in-line" in a single-mode fiber (SMF). Because amplification occurs without path separation, the pump, signal, and amplified idler encounter the same environmental phase changes, allowing stable phase regeneration without a PLL [21]. This results in an observed phase reduction of up to 56% and up to 11 dB gain at $10^{-5}$ bit error rate (BER) for a 10 Gb/s signal. This Letter also examines the regeneration system performance using different types of HNLFs and signal under different types of phase noise. System stability and sensitivity to tuning the BA pump power and frequency are also added.

The concept of an all-optical BPSK regenerator using Brillouin amplification is shown in Fig. 1. A BPSK signal (S), which is degraded with phase noise, such that $\phi_{\text{signal}} =$

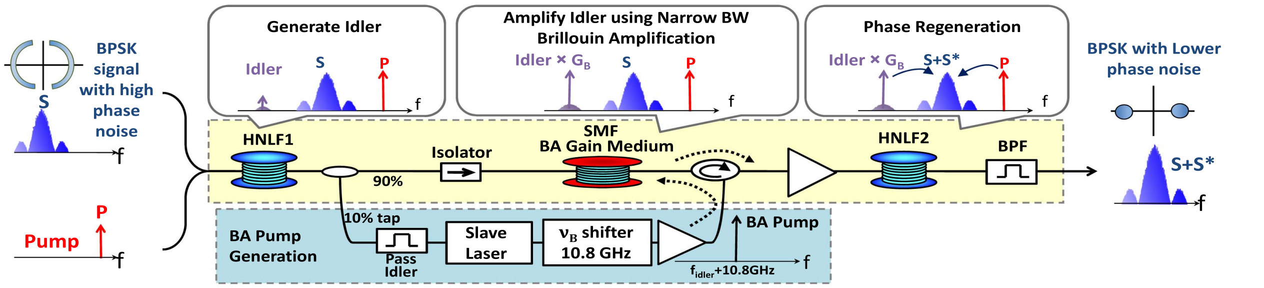


**Fig. 1.** Concept of BPSK regeneration without a phase-locked loop using narrow bandwidth Brillouin amplification (BA) to amplify the idler "in-line." The idler is generated in HNLF1 and exclusively amplified in an SMF using a counterpropagating Brillouin pump. Because the idler is amplified in the same path in which the signal and the pump propagate, their phase relationships remain fixed; avoiding the need for phase stabilization. Finally, the BPSK signal is regenerated in HNLF2 when $S^*$ is created and coherently added the signal. The Brillouin pump is generated by frequency up-shifting the slave laser CW output by 10.8 GHz; the slave laser is used to ensure stable frequency locking between the idler and BA pump. (P, pump; S, signal; $G_B$, Brillouin amplifier gain; BA, Brillouin amplifier.)

$\phi_{data} + \phi_{noise}$ and $\phi_{data}$ is either 0 or $\pi$, is combined with a CW pump (P) and both are sent into HNLF1 to generate a data pattern-free idler with the phase $\phi_{idler} = 2\phi_{signal} - \phi_{pump} = 2\phi_{noise} - \phi_{pump}$ (i.e., BPSK signal's second harmonic). The HNLF1 output is split into two paths using a 90/10 coupler. On the 10% tap, the appropriate frequency-locked Brillouin pump is generated by setting a slave laser to frequency lock to the tapped idler. The slave laser output is then frequency up-shifted by $\nu_B$, amplified, and sent into the SMF as a counterpropagating BA pump, where $\nu_B$ is the Brillouin gain frequency shift of a SMF and ≃10.8 GHz. On the 90% path, the idler is amplified in the SMF with gain ($G_B$) using the counterpropagating Brillouin pump, such that the idler acts as the Brillouin probe [16–20]. Because the idler is amplified in the SMF without path separation from the signal and pump, its phase remains locked to the signal and pump. The BA pump generation configuration using the slave laser guarantees frequency-locked Brillouin interaction. Since the BA is narrow BW, it acts as a filter that amplifies only the central frequency components of the idler. After propagating through the SMF, the pump, the signal, and the amplified idler are additionally amplified by an erbium-doped fiber amplifier (EDFA) and sent into HNLF2 for phase regeneration. In the phase regeneration stage, the signal phase is squeezed when the signal conjugate ($S^*$) is created through four-wave mixing as $\phi_{S*} = \phi_{pump} + \phi_{idler} - \phi_{signal}$ and constructively added to the signal. The output is thus proportional to $S + S^*$ and the phase noise effect on the modulated BPSK data channel would be reduced.

The experimental setup is depicted in Fig. 2(a). A 1 kHz line width laser at 1550.7 nm is modulated with BPSK-non-return-to-zero data at 10–30 Gb/s using a $2^{31-1}$ pseudo-random bit sequence pattern in a Mach–Zehnder modulator (MZM). The phase noise is loaded using a phase modulator driven with a 1 GHz tone or white noise for various experiments. The signal and a CW pump at 1552.4 nm are amplified, combined in a 50/50 coupler, and both sent into a 357 m HNLF1 (ZDW = 1545 nm), in which the signal and pump power levels are set at 18.6 and 17.1 dBm at the HNLF1 input, respectively. The signal and pump lasers are independent and each laser has a wavelength stability of ±50 MHz over 1 h. The HNLF1 output is split into two paths using a 90/10 coupler. On the 90% arm, a liquid crystal on silicon (LCoS) filter is used to adjust the power levels and align relative phases, and its output is sent into the 500 m SMF BA gain medium. On the 10% arm, the slave laser output is frequency up-shifted in a MZM biased at null and fed with a $\nu_B = 10.821$ GHz tone (which yields the best gain for a BA). A sharp filter is then used to pass only the upper tone needed for Brillouin amplification, which is boosted in an EDFA5 and filtered before reaching the 500 m SMF. The path loss between the EDFA5 and the 500 m SMF is ~6 dB and the EDFA5 output is set at 26.1 dBm. The BA pump power is operated at nearly the stimulated Brillouin scattering (SBS) threshold of the 500

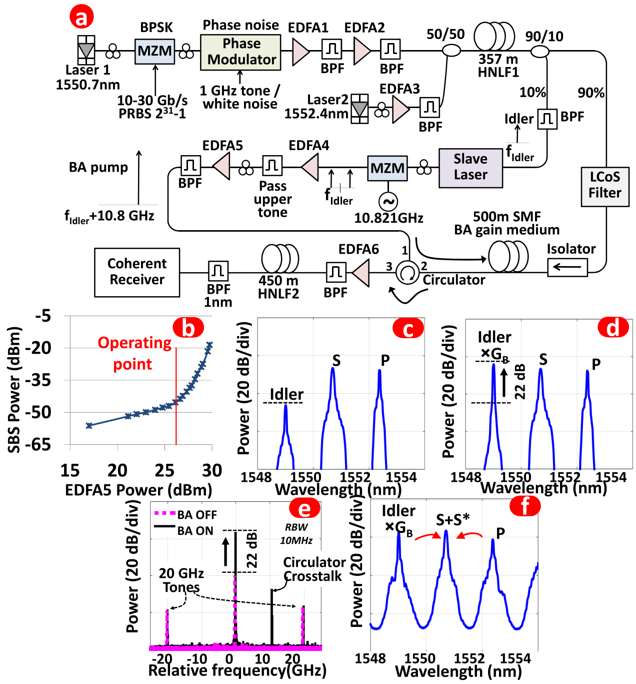


**Fig. 2.** (a) Experimental setup of BPSK regeneration using a BA. (b) SMF SBS performance as a function of EDFA5 output power (BA pump power) to illustrate the operating point. (c) Spectrum at the 500 m SMF input. (d) Spectrum at the 500 m SMF output with idler amplification. (e) Spectrum of the idler of a 20 Gb/s signal recorded at EDFA6 input using a 10 MHz resolution OSA without loading the phase noise. (f) Spectrum after regeneration at HNLF2 output.

SMF, as demonstrated in the SBS plot of the 500 m SMF as EDFA5 power varies, as shown in Fig. 2(b). The spectra before the BA [see Fig. 2(c)] and after the idler amplification [see Fig. 2(d)] show an idler gain of $G_B \simeq 22$ dB. The idler's spectrum at EDFA6 input is captured using a 10 MHz resolution optical spectrum analyzer (OSA), as shown in Fig. 2(e), when the signal is not loaded with phase noise. The spectrum shows that only the idler's central frequency is subject to gain. Yet the 20 GHz tones (originating from the periodicity of the data pattern) remain without gain. Circulator cross talk was observed between ports 1 and 3, as well as possible pump reflection on the optical connector between port 2 and the SMF, which together induce a tone with ~30 dB less power than the idler at port 3. The pump, signal, and amplified idler are amplified in EDFA6, set to 29 dBm, and sent into the regeneration stage of a 450 m HNLF2 (ZDW = 1556 nm). Finally, the regenerated output signal is filtered and sent to an 80 Gsample/s coherent receiver for analysis. At the receiver, the circulator cross talk was too small on the RF spectrum. Additional cross talk reduction could also be achieved by adding a filter or using a better circulator.

Performance is characterized by varying the phase noise level and recording the constellations and error-vector-magnitude (EVM) values for 10 and 20 Gb/s signals, as shown in Figs. 3(a) and 3(b) at the system input and output. HNLF2 was replaced with a 500 m Furukawa dispersion-stable HNLF (ZDW = 1556 nm) to increase the SBS threshold of HNLF2 [22]. This would allow higher pumping power from EDFA6 to HNLF2, which improves the conversion and regeneration performance, as observed in Figs. 3(c)–3(e), by enabling creating $S^*$ with relatively close power to $S$. EDFA6 was set at 32.2 dBm, and the constellations were recorded for a 20 Gb/s signal, as shown in Fig. 3(c). The $\varphi_{\text{noise}}$ was changed from a tone to white noise; the latter was generated using amplified spontaneous emission and a photodiode, to roughly emulate the phase noise that could be accumulated in optical fiber links, and the performance was recorded for 20–30 Gb/s signals, as shown in Figs. 3(d) and 3(e). The improvements in EVM and in $\phi_{\text{noise}}$ are shown in Figs. 3(f) and 3(g), respectively, in which the $\phi_{\text{noise}}$ measurement is calculated by defining the phase noise deviation $[\delta(\theta)]$ between the two ends of a constellation [as shown in Fig. 3(a) input with level 4 phase noise] and calculating the percentage of its reduction after regeneration. For case (a) with 10 Gb/s and 1 GHz tone $\phi_{\text{noise}}$, the EVM improvement reaches 60.7% when the input EVM is 57.1%, but the EVM improvement for case (b) at 20 Gb/s does not exceed 48%. This degradation can be overcome with a better HNLF2, as shown in case (c). Also, loading broadband phase noise as in cases (d) and (e) would reduce the improvement gained from the regeneration system. We believe this happens because the white phase noise had power within the slave laser tracking range (±300 MHz, Eblana photonics 1550-NLW), unlike the previously examined 1 GHz noise tones, which consequently degraded the slave laser performance and BA gain.

BER improvement was evaluated for phase noises of level 1 and level 2 at 10 Gb/s, as shown in Fig. 4(a), and at 20 Gb/s, as shown in Fig. 4(b), corresponding to the cases (a) and (b) in Fig. 3. For the 10 Gb/s signal, prior to regeneration and at a BER of $10^{-5}$, level 1 phase noise caused the eye to degrade with at least a 12 dB penalty compared to the clean back-to-back signal, and level 2 noise caused a 2 dB degradation. After regeneration, improvement at level 1 reached 11 dB and level 2 improvement was 1.5 dB. For the 20 Gb/s channel, level 1 $\phi_{\text{noise}}$ introduced a penalty of 14 dB and the regeneration reduced that by 9.1 dB, and for level 2 the penalty was 2.8 dB and the regeneration system improved this by 1.5 dB at the BER of $10^{-5}$.

Figure 5 indicates the impact of tuning different parameters on the regenerator stability and performance for the 10 Gb/s signal at phase noise of level 2 degraded with the $\phi_{\text{noise}}$ of 1 GHz tone. In Fig. 5(a), the BA frequency shifter is manually varied from the optimal $\nu_B$ by tuning the synthesizer feeding the MZM shifter, and the EVM of the output signal is recorded. When the BA frequency drifts, gain on the idler decreases and its phase might change, both of which degrade regeneration performance. Although the regeneration setup lowers the EVM from 51.7% to 20.3%, the EVM after

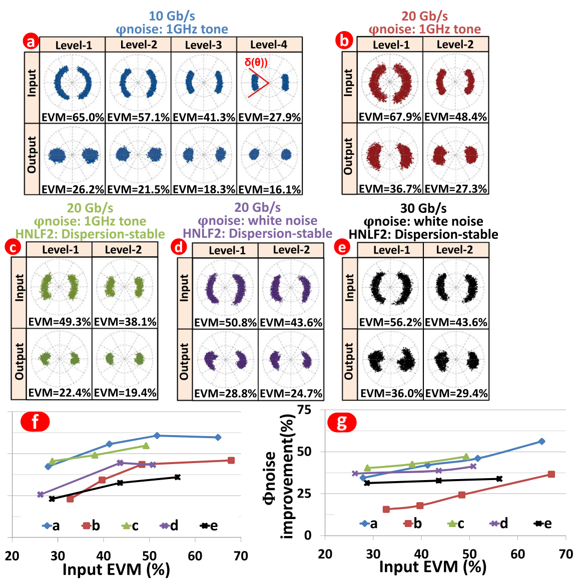


**Fig. 3.** (a)–(e) Constellations before and after the phase-sensitive regeneration system at different bitrates ranging between 10 and 30 Gb/s with different phase noise levels, different types of HNLF2, and different types of phase noise (1 GHz tone or white noise). (f) EVM percentage of improvement for the various scenarios in (a)–(e). (g) Percentage of improvement in the $\phi_{\text{noise}}$ for the different scenarios.

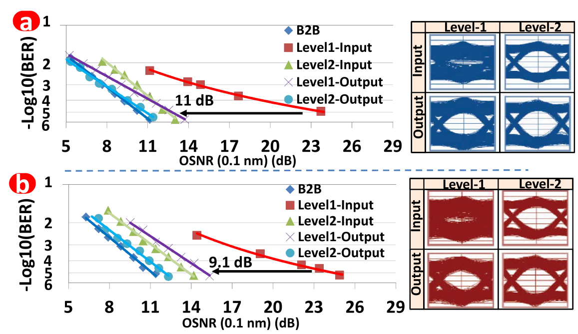


**Fig. 4.** BER performance and corresponding eyes before and after the regeneration system when $\phi_{\text{noise}}$ is 1 GHz tone for signals at: (a) 10 Gb/s, and (b) 20 Gb/s [same cases (a) and (b) in Fig. 3 for level 1 and level 2].

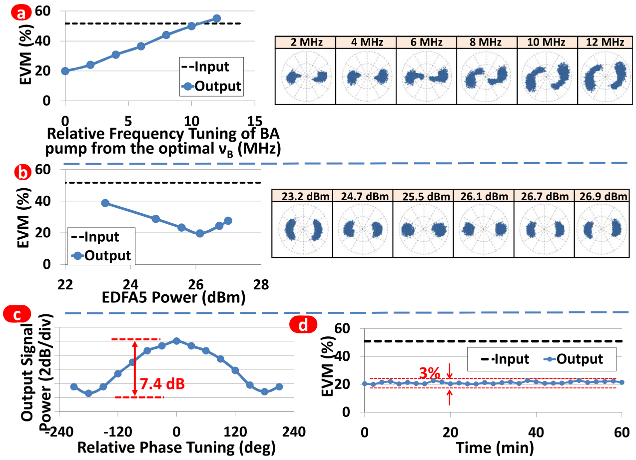


**Fig. 5.** Experimental study of tuning various parameters on system performance and its stability when regenerating a 10 Gb/s signal with $\phi_{\text{noise}}$ of level 2: (a) effect of tuning the BA pump frequency from the optimal $\nu_B$ and recording the EVM and constellations of different frequency tunings cases. (b) Effect of tuning the BA gain through tuning BA's pump power (EDFA5 power) on the EVM, showing the regeneration output constellations at different EDFA5 power levels. (c) Measurement of the PSDR. (d) System EVM performance over an hour while running the system without PLL feedback.

regeneration might exceed the EVM of a noisy input signal if the idler and the Brillouin amplifier pump frequencies drift by 10 MHz. The BA pump power was adjusted by tuning the power of EDFA5 and the EVM and constellations were recorded, as shown in Fig. 5(b). The output EVM indicates that the optimal performance was achieved when the BA pump power was set to 26.2 dBm; the idler had almost the same power as the signal and pump for the best conversion at HNLF2. Further increase of the pump power would introduce power mismatch and drive the BA to operate above the SBS threshold with higher added spontaneous noise and worse output EVM. The phase of the idler was tuned on the LCoS filter and the phase-sensitive dynamic range (PSDR) was measured at 7.4 dB for the 10 Gb/s signal with the level 2 of $\phi_{\text{noise}}$. Stability was examined, as shown in Fig. 5(c), by setting the system to its optimal configuration and letting the system run without feedback for an hour, after which the EVM varied by 3 percentage points.

In conclusion, this Letter describes the experimental demonstration of a PSA-based BPSK channel phase regeneration system without a PLL by applying in-line idler amplification using a Brillouin amplifier. We found that using nonlinear elements with higher conversion efficiency and higher SBS threshold can help achieve better results and that the regeneration system could be more useful in environments with higher phase noise.

We believe that BA amplification of the idler in-line should be insensitive to the bitrate. However, this approach could be limited by other different parameters. For example, Brillouin interaction is a polarization-sensitive process, which should be considered for practical deployment. In addition, $\nu_B$ is temperature dependent [20], and may need to be optimized and carefully managed. Additionally, Brillouin interaction spontaneous noise depends on the input signal and pump power levels [20]. In this experiment, we optimized these parameters to maximize the amplified idler central frequency power compared to the phase noise spectral components while minimizing BA noise. For practical implementations, input power levels may be so low that the added BA noise may overwhelm the phase noise reduction. We anticipate that this approach is thus useful where input power is sufficiently high.

**Funding.** Center for Integrated Access Network (CIAN) (Y501119); National Science Foundation (NSF) (ECCS-1202575); Defense Security Cooperation Agency (DSCA) (4440646262); Fujitsu Laboratories of America (FLA).

## REFERENCES

1. J. P. Gordon and L. F. Mollenauer, Opt. Lett. **15**, 1351 (1990).
2. K. Croussore and G. Li, IEEE J. Sel. Top. Quantum Electron. **14**, 648 (2008).
3. R. Slavík, F. Parmigiani, J. Kakande, C. Lundström, M. Sjödin, P. A. Andrekson, R. Weerasuriya, S. Sygletos, A. D. Ellis, L. Grüner-Nielsen, D. Jakobsen, S. Herstrøm, R. Phelan, J. O'Gorman, A. Bogris, D. Syvridis, S. Dasgupta, P. Petropoulos, and D. J. Richardson, Nat. Photonics **4**, 690 (2010).
4. R. Slavík, A. Bogris, F. Parmigiani, J. Kakande, M. Westlund, M. Skold, L. Grüner-Nielsen, R. Phelan, D. Syvridis, P. Petropoulos, and D. J. Richardson, IEEE J. Sel. Top. Quantum Electron. **18**, 859 (2012).
5. T. Umeki, M. Asobe, H. Takara, Y. Miyamoto, and H. Takenouchi, Opt. Express **21**, 18170 (2013).
6. T. Richter, C. Meuer, R. Ludwig, and C. Schubert, in *Optical Fiber Communications Conference (OFC)* (2012), paper OM3B.4.
7. Á. Szabó, B. J. Puttnam, D. Mazroa, S. Shinada, and N. Wada, IEEE Photon. Technol. Lett. **24**, 2087 (2012).
8. S. Sygletos, P. Frascella, S. K. Ibrahim, L. Grüner-Nielsen, R. Phelan, J. O'Gorman, and A. D. Ellis, Opt. Express **19**, B938 (2011).
9. A. Lorences-Riesgo, C. Lundström, F. Chiarello, M. Karlsson, and P. A. Andrekson, in *European Conference on Optical Communication (ECOC)* (2014), paper Tu.1.4.3.
10. M. Ziyadi, A. Mohajerin-Ariaei, J.-Y. Yang, Y. Akasaka, M. Chitgarha, S. Khaleghi, A. Almaiman, A. Abouzaid, J. Touch, and M. Sekiya, in *Conference on Lasers and Electro-Optics (CLEO)* (2014), paper STu2J.3.
11. P. Frascella, S. Sygletos, F. C. G. Gunning, R. Weerasuriya, L. Grüner-Nielsen, R. Phelan, J. O'Gorman, and A. D. Ellis, IEEE Photon. Technol. Lett. **23**, 516 (2011).
12. T. Kurosu, M. Gao, K. Solis-Trapala, and S. Namiki, Opt. Express **22**, 12177 (2014).
13. H. C. H. Mulvad, F. Da Ros, M. Galili, K. Dalgaard, and L. K. Oxenløwe, J. Lightwave Technol. **33**, 2189 (2015).
14. M. R. Chitgarha, S. Khaleghi, M. Ziyadi, A. Mohajerin-Ariaei, A. Almaiman, W. Daab, D. Rogawski, M. Tur, J. D. Touch, C. Langrock, M. M. Fejer, and A. E. Willner, Opt. Lett. **39**, 2928 (2014).
15. N. K. Kjøller, K. M. Røge, P. Guan, H. Christian, H. Mulvad, M. Galili, and L. K. Oxenløwe, J. Lightwave Technol. **34**, 643 (2016).
16. G. P. Agrawal, *Nonlinear Fiber Optics* (Academic, 2006).
17. W. Wei, L. Yi, Y. Jaouën, M. Morvan, and W. Hu, Opt. Express **23**, 19010 (2015).
18. L. Banchi, M. Presi, R. Proietti, and E. Ciaramella, Opt. Express **18**, 12702 (2010).
19. S. Sternklar and E. Granot, Opt. Lett. **28**, 977 (2003).
20. B. J. Eggleton, C. G. Poulton, and R. Pant, Adv. Opt. Photon. **5**, 536 (2013).
21. A. Almaiman, Y. Cao, M. Ziyadi, P. Liao, A. Mohajerin-Ariaei, C. Bao, F. Alishahi, A. Fallahpour, B. Shamee, A. J. Willner, N. Ahmed, Y. Akasaka, T. Ikeuchi, S. Wilkinson, M. Tur, and A. E. Willner, in *Optical Fiber Communication Conference (OFC)* (2016), paper W4D.5.
22. S. Takasaka, Y. Taniguchi, M. Takahashi, J. Hiroichi, M. Tadakuma, H. Matsuura, K. Doi, and R. Sugizaki, in *Optical Fiber Communication Conference (OFC)* (2014), paper W3E.2.